Boada-Acosta, YF.; Vignoni, A.; Picó, J. (2017). Engineered Control of Genetic Variability Reveals Interplay among Quorum Sensing, Feedback Regulation, and Biochemical Noise. ACS Synthetic Biology. 6(10):1903-1912. https://doi.org/10.1021/acssynbio.7b00087

Engineered control of genetic variability reveals interplay between quorum sensing, feedback regulation and biochemical noise

Yadira Boada,[†] Alejandro Vignoni,[‡] and Jesús Picó[*,†]

†*Institut d'Automàtica i Informàtica Industrial, Universitat Politècnica de València, Camino de Vera s/n, 46022, Valencia, Spain.*

‡*Center for Systems Biology Dresden, Max Planck Institute of Molecular Cell Biology and Genetics, Pfotenhaurstr. 108, 01307 Dresden, Germany.*

E-mail: jpico@upv.es

Abstract

Stochastic fluctuations in gene expression trigger both beneficial and harmful consequences for cell behavior. Therefore, achieving a desired mean protein expression level while minimizing noise is of interest in many applications, including robust protein production systems in industrial biotechnology. Here we consider a synthetic gene circuit combining intracellular negative feedback and cell-to-cell communication based on quorum sensing. Accounting for both intrinsic and extrinsic noise, stochastic simulations allow us to analyze the capability of the circuit to reduce noise strength as a function of its parameters. We obtain mean expression level and noise strength for all species under different scenarios showing good agreement with system-wide available experimental data of protein abundance and noise in *E. coli*. Our *in silico* experiments, validated by preliminary *in vivo* results, reveal significant noise attenuation in gene

expression through the interplay between quorum sensing and negative feedback, and highlight the differential role they play in regard to intrinsic and extrinsic noise.

Keywords

cellular noise, noise attenuation, protein expression control, quorum sensing, feedback control

Introduction

Noise is pervasive in the cellular mechanisms underlying gene expression (*1*). It propagates to downstream genes at the single cell level, and eventually causes variation within an isogenic population (*2*, *3*) that may determine the fate of individual cells and that of a whole population (*3*, *4*).

At the gene level, noise can be traced back to intrinsic sources due to stochastic fluctuations in transcription and translation mechanisms, and extrinsic ones corresponding to gene independent fluctuations in protein expression due to external factors (*4*–*6*). To minimize the deleterious effects of noise, cells have evolved different strategies at the single-cell level: from different transcription and translation efficiency so as to reduce translation burst rates in key genes (*7*) to more elaborated strategies, such as negative feedback regulation to reduce noise by shifting the noise spectrum to a higher frequency region (*1*). Yet, cells live in communities, forming a population. At this level, extracellular signaling propagates intracellular stochastic fluctuations across the population (*8*). Thus, cells have adapted their communication mechanisms in order to improve the signal-to-noise ratio (*9*). One of such communication mechanisms is quorum sensing.

Quorum sensing (QS), initially discovered in *V. fisheri* and *P. putida*, is a cell-to-cell communication mechanism whereby bacteria exchange chemical signaling molecules, called autoinducers, whose external concentration depends on the cell population density. It is known that synchronization and consensus protect from noise (*10*). Cells detect a threshold

concentration of QS autoinducers and alter gene expression accordingly (*11*), driving the population as a whole to achieve a desired consensus gene expression level despite the individual noise of each member of the population. Cells consensus induced by QS is thought to reduce extrinsic noise by reducing the transmission of fluctuating signals in the low-frequency domain (*12*), enhances intrinsic stochastic fluctuations (*8*), and allows entrainment of a noisy population when faced to environmental changing signals (*13*). Therefore QS seems an effective tool to control the phenotypic variability in a population of cells (*9*).

Phenotypic variability has important practical relevance in many applications in the areas of biomedicine, biotechnology and other branches of biological science (*14*) as the presence of heterogeneous subpopulations may have significant impact on the yield and productivity of industrial cultures (*15–17*). Thus, improving homogeneity of protein expression in industrial cultures is a goal of economic relevance for microbial cell factory processes that has traditionally been attempted either by optimizing environmental conditions in the culture or by careful selection of the strain. Open loop strategies based on sensitivity analysis have been used to provide guides as to how properly tune transcriptional and translational parameters so that the noise levels can be controlled while the mean values can be simultaneously adjusted to desired values (*18*). While sensitivity analysis gives very valuable insights, open loop control is not robust against system uncertainty and/or variations. There is an ever-growing appreciation that biological complexity requires new bioprocess design principles.

Synthetic biology, sometimes defined as the engineering of biology, has the potential to engineer genetic circuits to perform new functions for useful purposes in a systematic, predictable, robust, and efficient way (*19*). In the last years, several synthetic circuits have been proposed with the ultimate goal of dealing with gene expression noise (*20*, *21*). Though circuits using negative feedback have been proved to decrease gene expression noise (*22*), single-cell intracellular feedback loops do not take into account that in practice one is interested in controlling gene expression mean value and noise across a population of cells. Feedback across a population of cells can be implemented by means of quorum sensing-

based strategies, and has been shown to reduce noise effects (*9*, *12*, *23*). Indeed, cell-to-cell communication by means of quorum sensing induces consensus among cells (*24*), that is, contributes to reduce the difference of internal state among cells in a population. This, in turn, may contribute to protect from noise (*10*). Thus, the idea of joining both intracellular negative feedback and extracellular feedback via quorum sensing is a natural one, that has been suggested in (*25*, *26*).

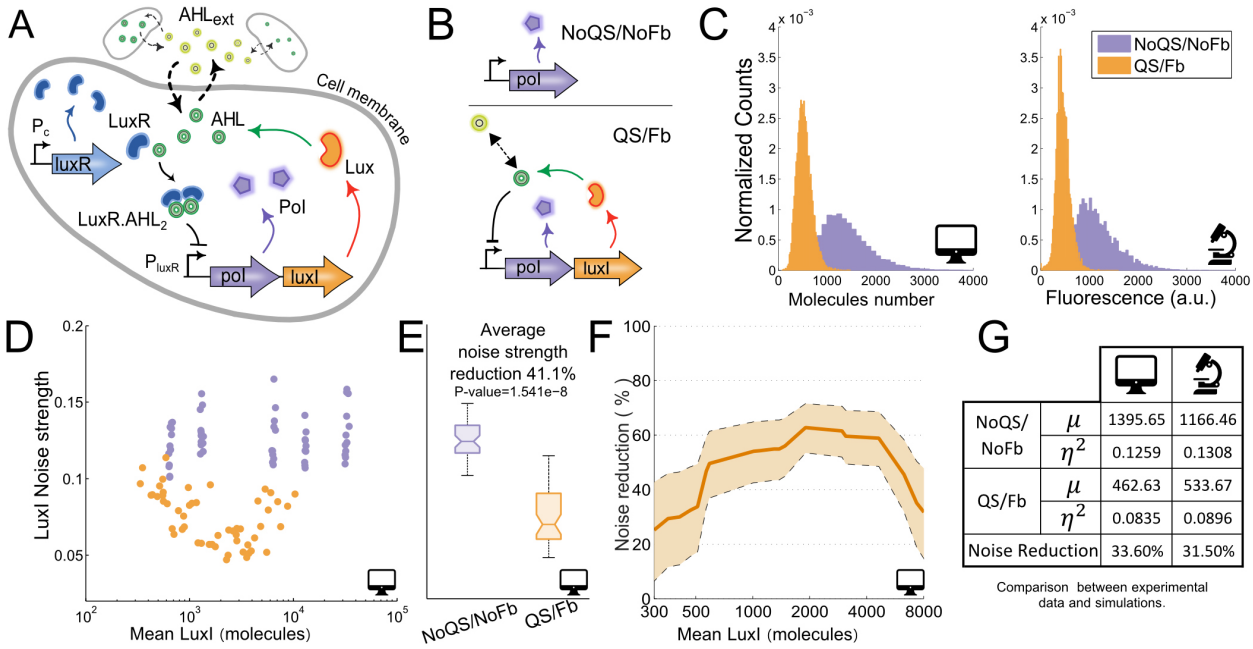

Figure 1: LuxI noise strength under presence/absence of quorum sensing and negative feedback. (A). Proposed synthetic gene circuit. (B) Circuits topologies: NoQS/NoFb (top) and QS/Fb (bottom). (C) Representative computational (left) and experimental (right) population histograms of LuxI noise strength for QS/Fb (orange) presenting a narrower gaussian-like distribution as compared to the Poisson-like one of NoQS/NoFb (purple). From computational simulations: (D) Sampled combinations of LuxI expression parameters for fixed LuxR ones show larger values of LuxI noise strength *vs.* mean for NoQS/NoFb (purple dots) than for QS/Fb (orange dots). (E) The QS/Fb circuit significantly reduces the average noise strength for the sampled parameters space by 41%, from $\langle \eta^2_{\mathrm{NoQS/NoFb}} \rangle = 0.1263$ down to $\langle \eta^2_{\mathrm{QS/Fb}} \rangle = 0.0744$. (F) For varying LuxI parameters the average reduction of noise strength in LuxI ranges from 30 % up to 60 % and shows dependence on the mean expression level. Data shown for LuxI means between the biotechnological relevant range $[300, 8000]$ molecules/cell. (G) Comparison of experimental and computational statistical moments.

In this work we analyze the synthetic gene circuit depicted in Fig 1A, designed to reduce gene expression noise while achieving a desired mean expression level in a protein of

interest (*25*). The circuit uses the repressible promoter P_{lux} designed in (*27*) to implement a negative feedback loop over the gene of interest, and adds a QS mechanism based on N-acyl-L-homoserine lactone (AHL) (*11*, *28*) to induce population consensus (Methods, Circuit description). We used the stochastic Chemical Langevin Equation (*29*) to explore the impact of some key circuit parameters on noise strength (Methods, Mathematical model and Computational analysis). To assess the role played by feedback and QS we compared the proposed circuit, denoted as QS/Fb, with constitutive expression (NoQS/NoFb) (Fig. 1B), and with a circuit with feedback but no quorum sensing (NoQS/Fb). Extrinsic noise was modeled by randomizing values of the model parameters (*30*, *31*). Our *in silico* analysis reveals significant noise attenuation in gene expression through the interplay between quorum sensing and negative feedback, and explain their different roles for different noise sources, highlighting the need for proper characterization of extrinsic noise. Preliminary *in vivo* results agree with the computational ones.

Results and discussion

Quorum sensing and negative feedback attenuate gene expression noise

We first addressed the question whether the proposed QS/Fb circuit effectively reduces noise strength with respect to the circuit NoQS/NoFb (Fig. 1B). The last one consists of the LuxR expression on the one hand, and the protein of interest (PoI) downstream the P_{lux} repressible promoter, without the luxI gene coding for LuxI protein, on the other. Since no autoinducer AHL is neither produced nor externally introduced, there is no repression, so the expression of PoI is essentially a constitutive one (Methods, Circuit description). This corresponds to the Poisson distribution observed in the purple population histogram in the left panel of Fig. 1C. Contrarily, the QS/Fb histogram departs from the Poisson distribution to become a narrow Gaussian-like one in the orange population histogram in the left panel of Fig. 1C.

This fact, and the reduction in the mean expression value, indicate the strong presence of regulation. In both cases we used the nominal circuit parameters (SI Table S1).

Reduction in noise strength was not due to a particular choice of the circuit parameter values, but a property of the proposed topology. Fig. 1D depicts LuxI noise strength *vs.* mean expression for 60 different combinations of the P_{LuxR} characteristics for both QS/Fb (orange points) and NoQS/NoFb (purple points). The points in the figure correspond to the mean values across the cells population for each combination of parameters (Methods, Computational analysis). The magnitude of noise strength reduction was larger for medium values of mean protein expression. Noise strength levels were similar for all mean expression values in the case of the NoQS/NoFb circuit. Mean expression values in this case depend only on the translation rate p_I for which five discrete values were used, inducing the five mean values seen in the figure. On the contrary, the QS/Fb circuit showed lower values of noise strength and more graded values of the mean expression level, as it depends on the combination of all three parameters varied.

More important, noise strength was consistently lower for the QS/Fb circuit. Taking together all the different combinations of promoter parameters for each circuit, and the average noise strength was significantly reduced by 41% in the presence of quorum sensing and negative feedback as shown in Fig. 1E.

For the given fixed LuxR expression parameters, the noise strength reduction in LuxI showed a clear dependence on its mean expression level. In Fig. 1F the minimum and maximum values of LuxI noise reduction are plotted as a function of its mean value. In the range between 600 and 6000 LuxI molecules it was possible to reduce the noise variance at least in 35% in the worst case scenario, with a maximum reduction of around 70% for means between 2000 and 3000 molecules. Changing the parameters of LuxR protein expression showed a trend consistent with the findings in (*12*): the higher values of translation p_R and degradation d_R are, the larger the noise reduction is (Fig 5; and SI Section S.7).

Experimental results confirm computational predictions

Experimental implementation of the proposed QS/Fb circuit would not only allow a preliminary experimental validation of its capability to reduce noise strength, but would also further validate the model parameters used throughout this study. To this end we experimentally implemented both the NoQS/NoFb and QS/Fb circuits (Methods, Strains and plasmids), and compared the experimental results with the computational ones (Supplementary information S.10). As model parameters we used $p_I = 0.4\,\mathrm{min}^{-1}$, $k_{dlux} = 200$ molecules, $\alpha_I = 0.01$, $d_R = 0.07\,\mathrm{min}^{-1}$, $p_R = 4\,\mathrm{min}^{-1}$ (Methods, Mathematical model) and nominal values in (SI Table S1) otherwise.

The steady state population histograms of LuxI for the circuits QS/Fb (orange) and NoQS/NoFb (purple) under the same experimental conditions are depicted in Fig. 1C. The computational predictions are in the left panel, while the right panel shows flow cytometry experimental results. Both results were qualitatively comparable without any tuning, fitting or change in the model parameters. We only required a common scaling factor to convert from relative units of fluorescence to number of molecules (SI Section S.10).

The experimental results showed LuxI noise strength reduced by 31.5% meanwhile the computational simulations predicted a 33.6% reduction (Fig. 1G).

Feedback pays-off when extrinsic noise dominates

At this point the question arises as to what are the roles of quorum sensing and feedback in noise strength reduction, and what are their effects in view of both intrinsic and extrinsic noise.

To answer this question we first contextualized the computational results using available experimental data of noise strength and protein abundance in *E. coli*. We used experimental data taken from (*32*), and plotted it against our computational results in three scenarios: base control circuit with no quorum sensing or feedback (NoQS/NoFb, $k_A = 0$), our circuit with both quorum sensing and feedback (QS/Fb), and the hypothetical circuit with feedback

but without quorum sensing (NoQS/Fb, $D = 0$). For each scenario we considered different combinations of parameters with values of the mean protein number in the range $10^0 - 10^5$, (Methods, Computational analysis).

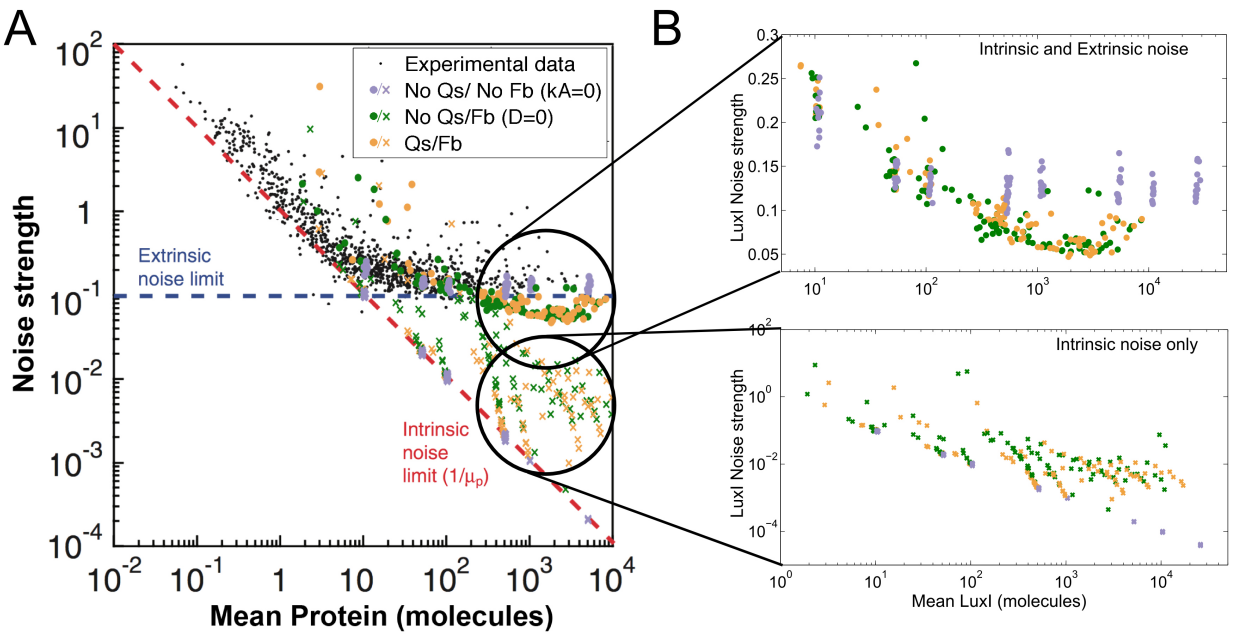

Figure 2: Comparison between experimental data and different scenarios evaluated computationally. (A) Experimental data of protein abundance and noise in *E. coli* taken from (*32*) is plotted as black dots. The dashed red and blue lines are the intrinsic noise limit and the extrinsic noise limits respectively, taken from the same reference. Simulations of the gene circuits in our study, including both intrinsic and extrinsic noise, are plotted using purple dots (NoQS/NoFb), green (NoQS/Fb) and orange ones (QS/Fb). Simulations including only intrinsic noise are plotted as crosses: violet (NoQS/NoFb), green (NoQS/Fb) and orange (QS/Fb). (B) Zoom of the scenarios considering both intrinsic and extrinsic noise (top) and only intrinsic noise (bottom).

Fig. 2A shows the experimental data plotted as black dots. The dashed red and blue lines are the intrinsic and extrinsic noise limits respectively, taken from the same reference above. Simulations including both intrinsic and extrinsic noise are plotted as purple dots (NoQS/NoFb), green (NoQS/Fb) and orange ones (QS/Fb) using the same data as in Fig. 1C. Our computational results were in good agreement with the experimental data and derived limits in (*32*). The results corresponding to the base control circuit NoQS/NoFb clearly were over the noise limits.

Unexpectedly, noise strength of both circuits QS/Fb and NoQS/Fb showed very similar behavior. As shown in the upper panel of Fig. 2B the QS/Fb and NoQS/Fb points lay in the same region. For medium and high mean protein expression values noise strength in QS/Fb and NoQS/Fb decreased just below the reported extrinsic noise limit, and well below the noise strength for the base NoQS/NoFb circuit. Though high protein expression are of main interest for the intended application of our circuit in an industrial biotechnological context of heterologous protein production, we were also interested in the performance of the circuits at low mean protein numbers. Interestingly, the situation in this region was reversed. The open loop circuit NoQS/NoFb showed consistent lower noise strength values than QS/Fb and NoQS/Fb. Therefore, feedback contributed to reducing noise strength for medium-high protein expression where extrinsic noise dominates.

Quorum sensing helps feedback to cope with intrinsic noise

The last result was inconclusive about the contribution of quorum sensing to reduce noise strength. To settle this issue we concentrated our analysis in the medium-high protein expression region where feedback contributed to reduce noise strength and extrinsic noise dominates.

We first wanted to elucidate whether QS mainly contributed reducing the intrinsic component of noise. If this was the case, its effect could be masked by the dominant extrinsic noise. To that end we carried out simulations for the same combinations of parameters as before, but suppressing extrinsic noise, and considering the three scenarios NoQS/NoFb, QS/Fb, and NoQS/Fb. The results are shown in Fig. 2A, plotted as violet (NoQS/NoFb, $k_A = 0$), green (NoQS/Fb, $D = 0$) and orange crosses (QS/Fb). The bottom panel of Fig. 2B shows a zoom into the relevant region. Introducing either feedback alone or feedback plus quorum sensing increased noise strength values with respect to the minimal base control circuit representing plain constitutive protein expression. The results for this base NoQS/NoFb circuit were along the intrinsic noise limit (*32*). These results were consistent

with the findings at low mean protein values where intrinsic noise dominates. The circuit NoQS/Fb with feedback and no cell-to-cell communication showed higher values of noise strength, specially for lower values of mean protein number. Finally, reintroducing quorum sensing (QS/Fb) was able to slightly improve noise strength.

To confirm this result we assessed the difference between the LuxI noise strength values for each combination of parameters in both circuits QS/Fb and NoQS/Fb. We measured noise strength reduction as $((1 - \eta^2_{\mathrm{NoQS/Fb}}/\eta^2_{\mathrm{QS/Fb}}) \cdot 100\%)$ and used it to obtain Fig. 3. First, we analyzed the case when only intrinsic noise is present as a function of circuit parameters associated to LuxI expression. As the LuxR parameters used before were close to be a best case scenario (see Fig 5) this time we used a smaller translation rate $\mathrm{p_R} = 2\,\mathrm{min}^{-1}$ corresponding to an average scenario. Fig. 3A shows the noise strength map difference for several combinations of the dissociation constant $\mathrm{k_{dlux}}$ *vs.* the LuxI translation rate $\mathrm{p_I}$ for a tight promoter $\mathrm{P_{lux}}$, $\alpha = 0.01$ and a leaky one $\alpha = 0.1$ in both noise scenarios. The noise strength reduction when QS was added reached a 100% for low values of $\mathrm{p_I}$. Increasing the dissociation constant improved noise reduction, specially for a leaky promoter.

The previous result suggested that the results reported in the literature showing a reduction in noise strength when QS was used were a result of modeling extrinsic noise as an additive signal. This hypothesis was confirmed when besides intrinsic noise we introduced an additive extrinsic noise to our system, with variance independent of the system states. Fig. 3B shows that in this case there also was a generalized noise strength reduction for most parameter combinations.

Finally, in case we restored extrinsic noise as parametric variability the results showed that adding QS may increase or decrease noise strength (Fig. 3C) strongly depending on the values of the circuits parameters, and suggesting that getting benefit of QS for medium-large mean expression values requires fine-tuning and optimizing the circuit parameters.

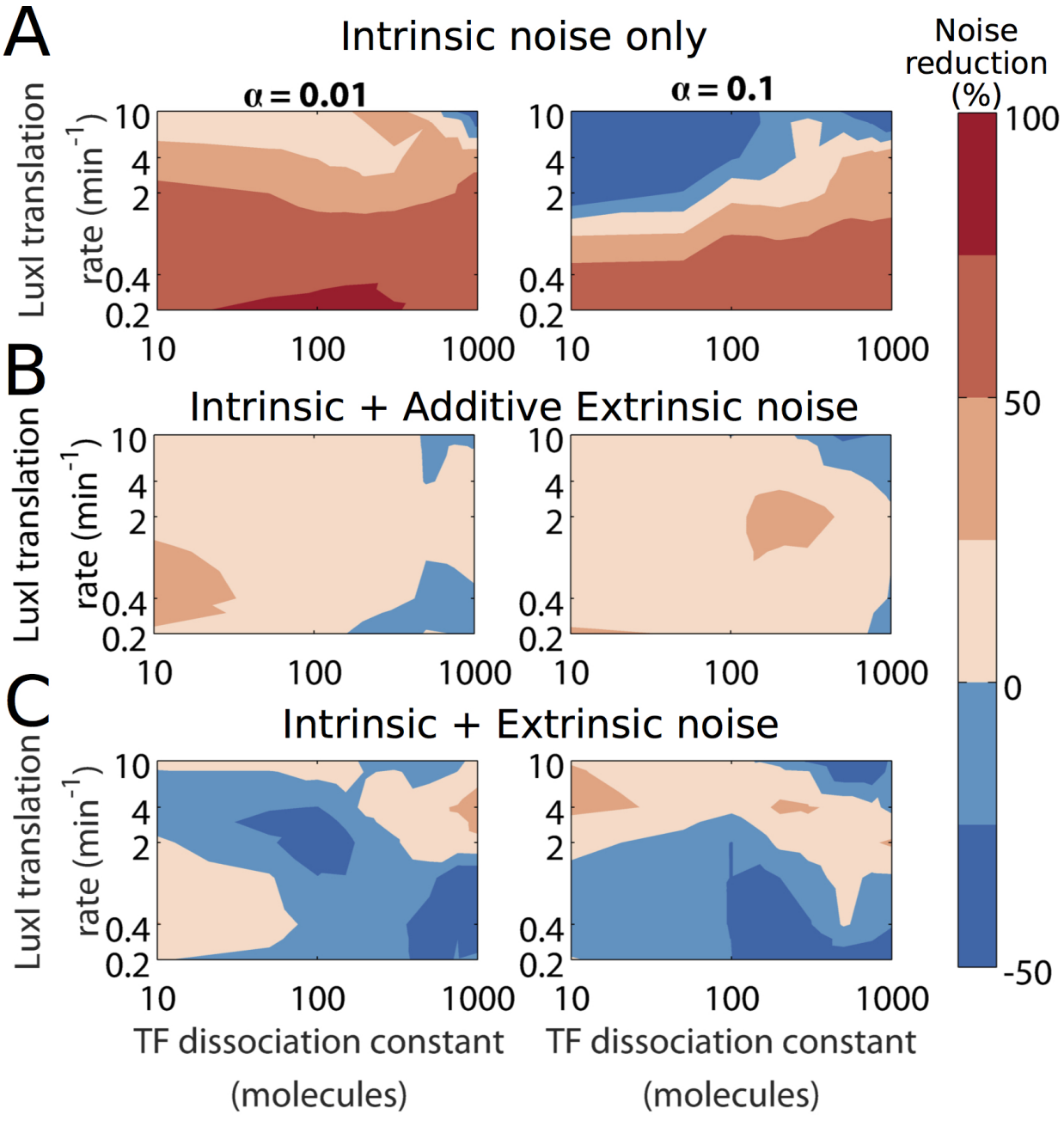

Figure 3: LuxI noise strength reduction as a function of circuit parameters. Color map of the reduction of LuxI noise strength when QS is added to Fb w.r.t. the dissociation constant k_{dlux} and the LuxI translation rate p_I. All other parameters were set to their values from (SI Table S1) . Left) Tight promoter $\alpha = 0.01$. Right) Leaky promoter $\alpha = 0.1$. (A) Only intrinsic noise is present. (B) Intrinsic noise and additive extrinsic noise. (C) Intrinsic and parametric extrinsic noise.

Tuning LuxI expression allows minimising noise-strength

Dependence of mean expression and noise strength on the Qs/Fb circuit parameters is a key factor to understand for the circuit to be of potential practical usage. To this end we performed thorough *in silico* experiments to estimate the noise strength and mean expression value of LuxI, as a proxy of the protein of interest, for different sets of the circuit parameters associated to LuxI expression (Methods, Computational analysis). We only evaluated two values for the basal expression, corresponding to a tight P_{lux} promoter ($\alpha = 0.01$), and a leaky one ($\alpha = 0.1$).

As for LuxR, we also considered two values corresponding to the scenarios we had before: a strong ribosome binding site (RBS) with ($p_R = 10\,\mathrm{min}^{-1}$) close to a best scenario for noise reduction, and a medium-weak RBS ($p_R = 2\,\mathrm{min}^{-1}$). We kept all other parameters to their nominal values (SI Table S1). Notice that although we considered variations in the translation rates p_I and p_R, in our model these are tantamount to consider equivalent variations in the lumped values of the corresponding products of protein burst size, transcription rate and gene copy number (Methods, Computational analysis).

Fig. 4 shows the noise strength map for different combinations of the dissociation constant k_{dlux} *vs.* the LuxI translation rate p_I when we consider both a tight promoter P_{lux}, $\alpha = 0.01$ (Fig. 4A) and or a leaky one $\alpha = 0.1$ (Fig. 4B). The means of LuxI protein number are shown as contour lines.

The mean expression levels of LuxI presented general monotonous trends in all cases. It increased for simultaneous rising of the dissociation constant and the LuxI translation rate. On the other hand, increasing leakiness of the LuxI promoter did tend to lower mean expression levels of LuxI for low values of the dissociation constant. Finally, using a weaker RBS controlling the translation of LuxR (Fig. 4B) produced a steeper increasing of the mean expression level as the dissociation constant and the LuxI translation rate increase.

Noise strength did not show simple patterns as a function of the circuit parameters. Larger variations between high and low noise strength values were observed for stronger

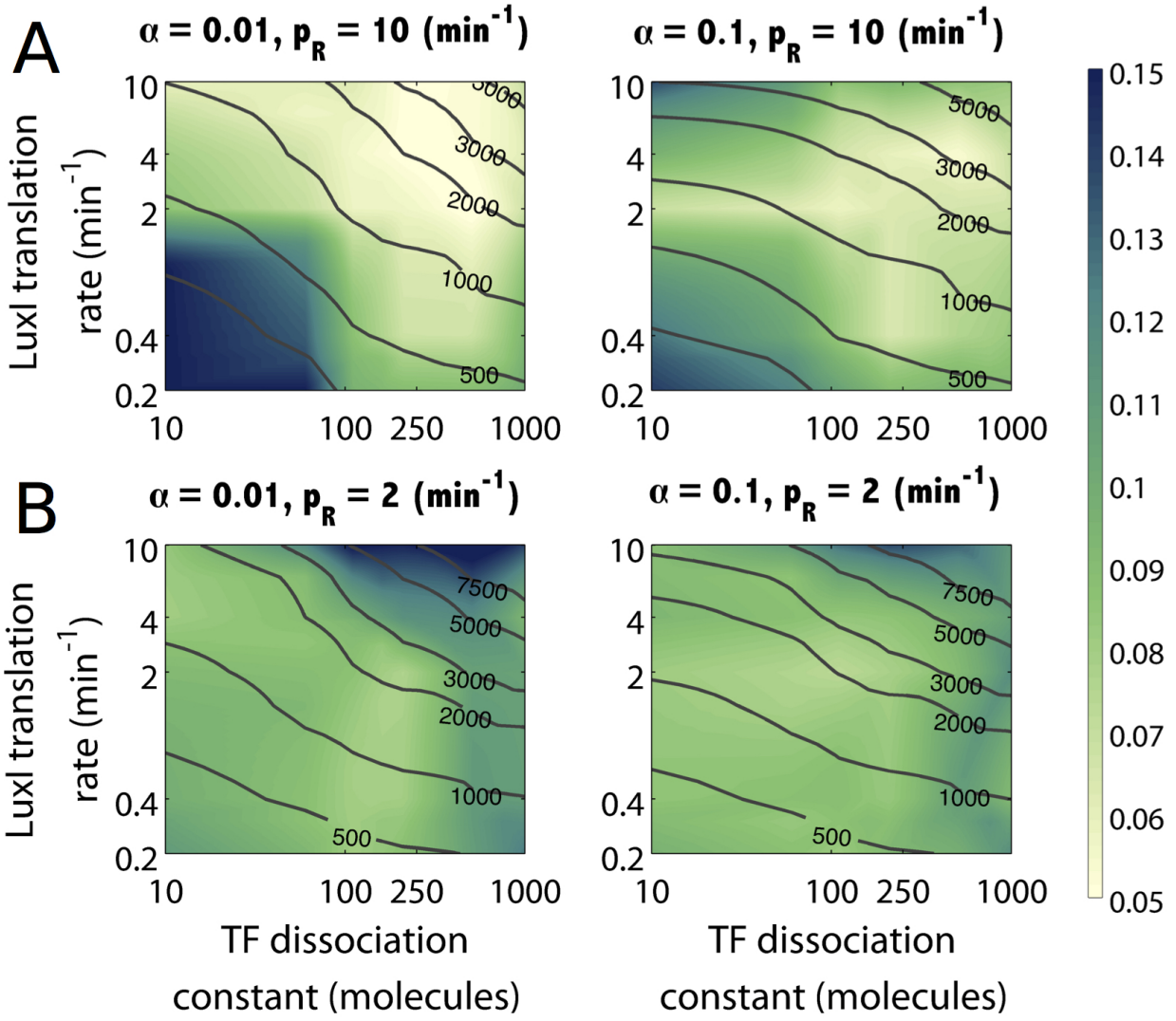

Figure 4: LuxI noise strength and mean as a function of circuit parameters. Color map of LuxI noise strength w.r.t. the dissociation constant k_{dlux} and the LuxI translation rate p_I. The level curves correspond to the mean number of LuxI molecules. (A) Strong LuxR RBS with $p_R = 10$ min^{-1}. (B) Medium-weak LuxR RBS with $p_R = 2$ min^{-1}.

LuxR RBS (Fig. 4A) independent of the leakiness of the promoter P_{lux}. In this case, the lowest values of noise strength were achieved for values of the dissociation constant k_{dlux} in the range $[100 - 500]$ molecules, and values of LuxI translation rate p_I in the range $[2 - 10]$ min^{-1}. The mean expression levels in this region were between $2 \cdot 10^3$ and $4 \cdot 10^3$ proteins, in agreement with the results shown in Fig. 1. Decreasing the LuxR RBS strength kept the the values of minimal noise strength essentially in the same region, but with higher values (Fig. 4B). The same trend towards higher values of noise strength was observed when the tight promoter P_{lux} was changed for a leaky one. This was more evident when a stronger LuxR RBS was used (Fig. 4A).

Fast LuxR turnover reduces LuxI noise strength

Finally, we analyzed the effect of LuxR expression parameters over LuxI mean expression level and its noise strength. In particular, we were interested in the effect of the LuxR translation rate p_R, as the main tuning knob of LuxI mean expression level, and the one of the degradation rate d_R.

On the one hand, LuxR synthesis rates proved to be a good sensitive tool to tune the desired LuxI mean expression level, with larger values of the last as the former decreased. Fig. 5 shows the LuxI noise strength maps and mean expression level curves as a function of values of the LuxR translation rate in the range 0.2 to 10 min^{-1}, and LuxR degradation rate in the range 0.02 to 0.2 min^{-1}. We fixed the LuxI translation rate to two values $p_I = 2\,min^{-1}$ and $p_I = 4\,min^{-1}$ around its nominal value, and considered both a tight P_{lux} promoter ($\alpha = 0.01$) and a a leaky one ($\alpha = 0.1$). All other parameters were kept to their nominal values described in (SI Table S1).

On the other hand, we confirmed that LuxI noise strength decreased with LuxR fast turnover. Unlike suggested in (*12*), the decrease is not uniform, having optimal values for d_R in the range 0.07 to 0.2 min^{-1} when LuxR translation rate p_R had medium to high values in the range 2 to 10 min^{-1} (SI Section S.7). The mean expression level was not very sensitive

to the LuxR degradation rate, with a slight increase as the degradation rate increased.

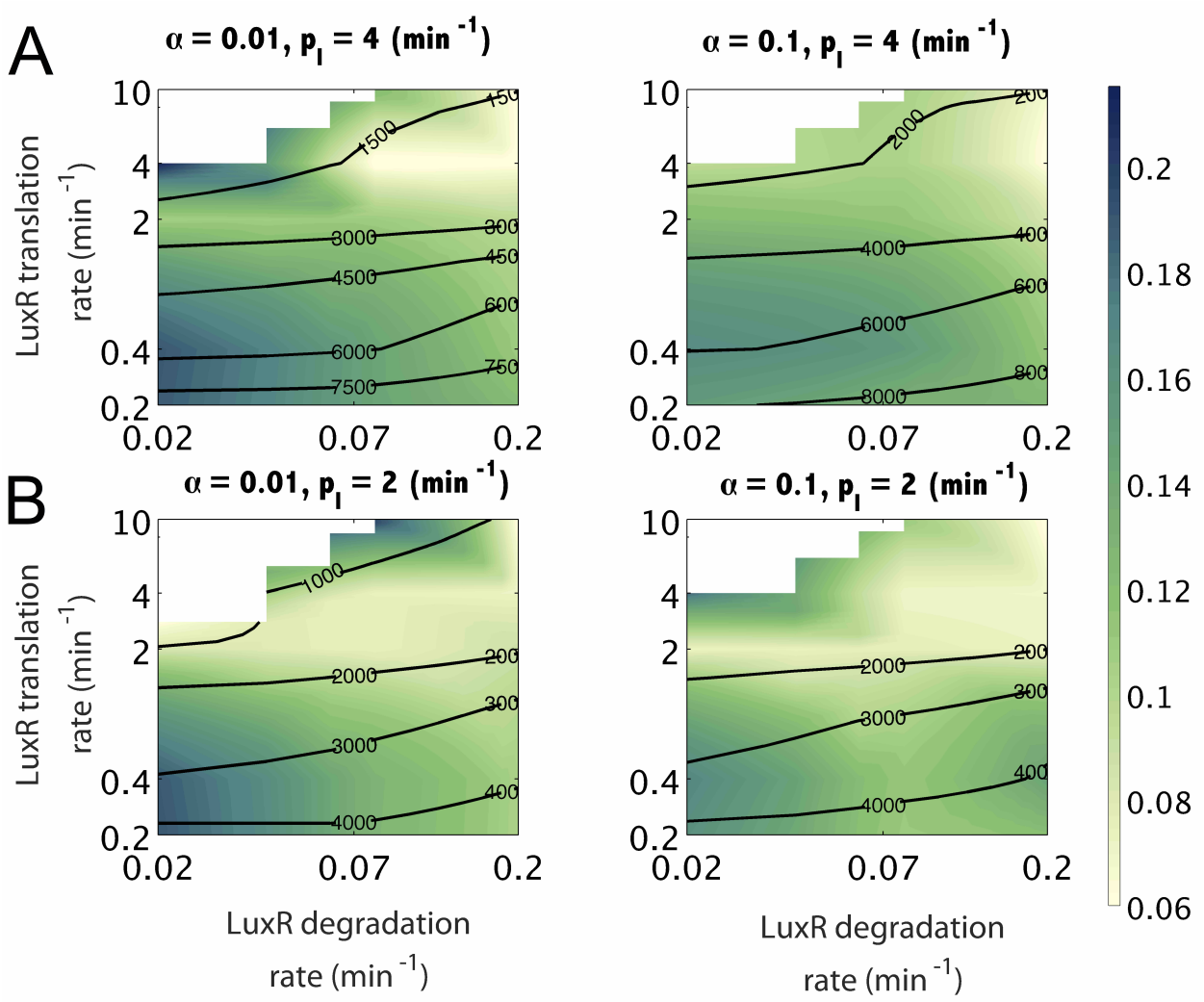

Figure 5: LuxI noise strength *vs.* LuxR parameters. LuxI noise strength maps and mean expression level curves for a tight P_{lux} promoter ($\alpha = 0.01$, top) and a a leaky one ($\alpha = 0.1$, bottom) with LuxI translation rates $p_I = 2\,\mathrm{min}^{-1}$ (left) and $p_I = 4\,\mathrm{min}^{-1}$ (right) around its nominal value.

Conclusion

Our results show that gene synthetic circuits benefiting from the interplay between feedback and cell-to-cell communication allow control of the mean expression level and noise strength of a protein of interest. A few circuit parameters easy to tune in the wet-lab can be used to

achieve noise strength reductions up to a 60% with respect to constitutive expression of the protein of interest.

Mean expression level and noise strength are not independent goals. At low mean values intrinsic noise dominates and sets the minimum noise strength attainable. At high mean values extrinsic noise dominates. Thus, there is a trade-off between expression level and noise strength, as revealed both by system-wide experimental data and theoretical analysis reported in the literature. Our computational results fitted well in this scenario, and suggest that tuning synthetic gene circuits to minimize noise while achieving a desired expression level will require a multi-objective optimization approach.

For high mean expression values we observed a clear benefit of having feedback as compared to constitutive expression. Even if achieving best noise suppression requires an optimal feedback tuning, as already seen e.g. in (*31*), noise reduction due to feedback was essentially structural, i.e. almost independent of its parameters, in this high mean expression region. Yet, adding quorum sensing on top of feedback did not decrease noise strength unless the circuit parameters are tuned. That is, the benefit from adding cell-to-cell communication is not just structural, but depended also on proper choice of the circuit parameters. This result is somewhat counter-intuitive and does not fully agree with previous works reporting a reduction of extrinsic noise in quorum sensing-based gene circuits, e.g. (*12*), that reported a structural benefit. This may be explained by the different approaches to model extrinsic noise. While we modeled it as parametric variability, most often extrinsic noise has been modeled as an additive stochastic signal essentially analogous to the intrinsic noise term. Thus, if we considered a scenario with intrinsic noise and no extrinsic one while keeping medium-high expression means, our results also showed an important reduction of noise strength when quorum sensing was added to feedback. Though the amount of reduction depended on the circuit parameters, we observed noise reduction for almost any combination of them. Moreover, if we considered additive extrinsic noise, we got qualitatively similar results to the ones when only intrinsic noise was present.

Given two different gene circuits, they will result in different noise because being different their physiological effect on the cell will be different. Yet, the chances that adding any extra random structure on top any given circuit results in a reduction of noise is extremely low. Thus, in the hypothetical scenario with no extrinsic noise we also found that adding either feedback or feedback and quorum sensing increased the noise strength with respect to the open loop constitutive gene expression circuit. This result might be explained by the increased complexity introduced by these circuits (*33*). The increased complexity introduced by the added circuit components will introduce extra randomness and variability, increasing noise. Yet, circuit complexity is not the only factor contributing. On the one hand, the circuit with quorum sensing and feedback achieved lower average noise strength values than the less complex only-feedback one in this scenario. On the other, when extrinsic noise was present constitutive expression was clearly noisier than any of the more complex QS/Fb and NoQS/Fb circuits for high protein mean expression values, though not for low ones where intrinsic noise dominates. Thus, the circuit complexity contribution to noise depends not only on its size, but in the interplay between size, noise structure, and circuit structure. An increased circuit complexity will increase noise unless the new feature can structurally reduce noise and it is properly tuned. Also, in the mean protein expression medium-high range of interest for industrial biotechnology, tuning circuit parameters in the circuit with both quorum sensing and feedback clearly allows coping with both intrinsic noise and extrinsic one, independently of its structure.

The experimental results, though preliminary, showed a high concordance the computational ones and confirmed the capability of the proposed circuit to reduce noise strength.

Methods

Circuit description

The synthetic gene circuit (Fig. 1A) combines two functional subsystems already implemented in *E. coli*. The first subsystem implements a cell-to-cell communication mechanism via quorum sensing, based on exchange of the small signaling autoinducer molecule N-acyl-L-homoserine lactone (AHL) (*11*, *34*). This autoinducer molecule passively diffuses across the cellular membrane to and from the external environment. Intracellular AHL is synthesized by the protein LuxI expressed by an homolog of the gene luxI of *V. fisheri* (*28*). The second subsystem uses the synthetic repressible promoter P_{lux} designed in (*27*) to control transcription of the gene *luxI*. This promoter is repressed by the transcription factor $(LuxR.AHL)_2$. Protein LuxR is expressed by gene *luxR* under the constitutive promoter P_c. Proteins LuxR and AHL bind creating the heterodimer (LuxR.AHL), which subsequently dimerizes forming the heterotetramer $(LuxR.AHL)_2$. This way, the negative feedback control of the LuxI expression is effectively implemented.

The circuit acts as a closed loop controller of the mean and variance of a protein of interest PoI. This protein can be either fused to protein LuxI, or coexpressed with it. In the first case, a linker is inserted between the fused proteins allowing intracellular self-cleavage using a TEV protease (*35–37*). Alternatively, if the protein of interest is coexpressed with LuxI, the controller will only act at the transcriptional level. In cases where transcriptional noise dominates translational one, e.g. when the average number of proteins made per mRNA transcript is larger than two (*38*), co-expressing LuxI with the protein of interest is a simple yet effective approach.

Mathematical model

To analyze how our genetic circuit affects intrinsic and extrinsic noise, we needed an appropriate model and a computationally efficient method. Both aspects are intertwined. We

considered an equivalent set of pseudo-reactions resulting from the deterministic model of the circuit, and then derived a stochastic model for a population of N cells whose mean corresponds to that of the deterministic one. We used the Chemical Langevin Equation approach (CLE). Though computationally much more efficient than the Chemical master equation (CME) or even the Gillespie algorithm, the CLE is still computationally demanding when the goal is to simulate a whole population of cells. Since the CLE approximates the CME by a system of stochastic differential equations of order equal to the number of species, a reduced deterministic model with as few species per cell as possible was desirable.

Reduced deterministic model

We aimed at obtaining a reduced model more amenable for computational analysis, but avoiding excessive reduction that would lead to lack of biological relevance. In particular, the species we obtained in the reduced model are not lumped ones. Reduced models accounting for total mRNA and total transcription factor have been proposed to match modeled species with measurable ones (*39*). In our case we explicitly modeled bound and unbound forms of the transcription factor, but the model accounts for the total LuxI protein. For our circuit this is a good proxy for the amount of protein of interest if both are co-expressed, and transcriptional noise dominates. In the best case, when the protein of interest is in self-cleavable tandem fusion with LuxI, both will express in 1:1 stoichiometric ratio (*36*). Moreover, the resulting lumped parameters in the reduced model are easy to associate to tuning knobs available in the wet-lab implementation in the relevant cases (*40*), and their values are amenable to be obtained experimentally.

Thus, in a first step we used the mass-action kinetics formalism (*41*) to get a deterministic model of the full reactions network corresponding to the genetic circuit (Supplementary information S.1). We then got a reduced order model by applying the *Quasi Steady-State Approximation* (QSSA) on the fast chemical reactions and taking into account invariant moieties (*42*, *43*) (SI Section S.2). The resulting deterministic reduced model is described

by equations (1)-(2).

$$
\begin{aligned}
\dot{n}_1^i &= \frac{\mathrm{C_I p_I}}{\mathrm{dm_I}}\left(\frac{\mathrm{k_{dlux}}+\alpha n_3^i}{\mathrm{k_{dlux}}+n_3^i}\right)-\mathrm{d_I}n_1^i \\
\dot{n}_2^i &= \frac{\mathrm{C_R p_R}}{\mathrm{dm_R}}+\mathrm{k_{-1}}n_6^i-\left(\frac{\mathrm{k_{-1}}}{\mathrm{k_{d1}}}n_4^i+\mathrm{d_R}\right)n_2^i \\
\dot{n}_3^i &= \frac{\mathrm{k_{-2}}}{\mathrm{k_{d2}}}(n_6^i)^2-(\mathrm{k_{-2}}+\mathrm{d_{RA_2}})n_3^i \\
\dot{n}_4^i &= \mathrm{k_{-1}}n_6^i+\mathrm{k_A}n_1^i+\mathrm{D}\left(\frac{\mathrm{V_{cell}}}{\mathrm{V_{ext}}}n_5-n_4^i\right)-\left(\frac{\mathrm{k_{-1}}}{\mathrm{k_{d1}}}n_2^i+\mathrm{d_A}\right)n_4^i \\
\dot{n}_5 &= \mathrm{D}\left(-N\frac{\mathrm{V_{cell}}}{\mathrm{V_{ext}}}n_5+\sum_{i=1}^{N}n_4^i\right)-\mathrm{d_{A_e}}n_5
\end{aligned}
\tag{1}
$$

with:

$$
n_6^i=\frac{\mathrm{k_{d2}}(\mathrm{d_{RA}}+\mathrm{k_{-1}})}{4\mathrm{k_2}}\left[\sqrt{\frac{8\mathrm{k_{-2}}(2\mathrm{k_{-2}k_{d1}}n_3^i+\mathrm{k_{-1}}n_2^in_4^i)}{\mathrm{k_{d1}k_{d2}}(\mathrm{d_{RA}}+\mathrm{k_{-1}})^2}+1}-1\right] \tag{2}
$$

where $\mathbf{n}(t)^i=[n_1(t)^i,n_2(t)^i,n_3(t)^i,n_4(t)^i,n_6(t)^i]^T$ is the vector of species LuxI, LuxR, $(\mathrm{LuxR.AHL})_2$, intracellular AHL and (LuxR.AHL) for the i^{th} cell respectively, and n_5 is the extracellular $\mathrm{AHL_{ext}}$.

Stochastic model

To model gene expression intrinsic noise we derived a stochastic CLE-based model whose mean corresponds to that of the deterministic reduced model (1)-(2). To this end we first considered the equivalent set of pseudo-reactions (3) for the deterministic model in the i^{th}

cell.

$$
\begin{aligned}
(\mathrm{LuxR}\cdot\mathrm{AHL})_2 &\xrightarrow{f(n_3,t)} \mathrm{LuxI} + (\mathrm{LuxR}\cdot\mathrm{AHL})_2\\
\mathrm{LuxI} &\xrightarrow{\mathrm{k_A}} \mathrm{LuxI} + \mathrm{AHL}\\
&\xrightarrow{\mathrm{tt_{LuxR}}} \mathrm{LuxR}\\
\mathrm{LuxR} + \mathrm{AHL} &\underset{\mathrm{k_{-1}}}{\overset{\mathrm{k_{-1}/k_{d1}}}{\rightleftarrows}} \mathrm{LuxR}\cdot\mathrm{AHL}\\
2(\mathrm{LuxR}\cdot\mathrm{AHL}) &\underset{g(n_6,t)}{\overset{g(n_6,t)}{\rightleftarrows}} (\mathrm{LuxR}\cdot\mathrm{AHL})_2\\
\mathrm{AHL} &\underset{\mathrm{DV_c}}{\overset{\mathrm{D}}{\rightleftarrows}} \mathrm{AHL_{ext}}\\
\mathrm{LuxI} &\xrightarrow{\mathrm{d_I}} \emptyset\\
\mathrm{LuxR} &\xrightarrow{\mathrm{d_R}} \emptyset\\
(\mathrm{LuxR}\cdot\mathrm{AHL})_2 &\xrightarrow{\mathrm{d_{RA_2}}} \emptyset\\
\mathrm{AHL} &\xrightarrow{\mathrm{d_A}} \emptyset\\
\mathrm{AHL_{ext}} &\xrightarrow{\mathrm{d_{Ae}}} \emptyset
\end{aligned}
\tag{3}
$$

where we denoted $f(n_3^i,t) \triangleq \frac{\mathrm{C_I p_I}}{\mathrm{dm_I}}\left(\frac{\mathrm{k_{dlux}}+\alpha_I n_3^i}{\mathrm{k_{dlux}}+n_3^i}\right)$ as the Hill-like function associated to LuxI expression, $g(n_6^i,t)$ corresponds to the dimerization reflected in equation (2), and $\mathrm{tt_{LuxR}} = \frac{\mathrm{C_R p_R}}{\mathrm{dm_R}}$ represent the transcription-translation activity of *luxI* and *luxR* respectively, $\mathrm{V_c} = \frac{\mathrm{V_{cell}}}{\mathrm{V_{ext}}}$ is the ratio between the cell volume and the culture medium volume, and $\emptyset$ denotes species degradation.

For the computational analysis we used the Euler-Maruyama discretization (4) of the stochastic model resulting from the set of pseudo-reactions (3) :

$$\mathbf{n}(t+\delta t) = \mathbf{n}(t) + \mathbf{S}\cdot\mathbf{a}(\mathbf{n})\delta t + \mathbf{S}\cdot\mathcal{N}\cdot\sqrt{\mathbf{a}(\mathbf{n})}\sqrt{\delta t}, \tag{4}$$

where $\mathbf{n}(t) = [\mathbf{n}(t)^i, \ldots \mathbf{n}(t)^{\mathrm{N}}, n_5]^T$ are the number of molecules of each species in the population. The stoichiometry matrix $\mathbf{S}$, whose elements are the stoichiometry submatrices for

each cell $\mathbf{S_{cell}}$ and the external stoichiometry $\mathbf{S_{ext}}$, has structure:

$$\mathbf{S} = \left[\begin{array}{c|c} \mathbf{S_{cell}} \otimes \mathbf{I_N} & \mathbf{0_{N\times 1}} \\ \hline \mathbf{S_{ext}} \otimes \mathbf{1_{1\times N}} & -1 \end{array}\right], \tag{5}$$

where $\otimes$ is the Kronecker product, $\mathbf{I_N}$ the identity matrix of dimension $N \times N$, $\mathbf{0_{N\times 1}}$ and $\mathbf{1_{1\times N}}$ are vectors of zeroes and ones respectively, and the coefficients in the stoichiometry matrices $\mathbf{S_{cell}}$ and $\mathbf{S_{ext}}$, obtained from the set of pseudo-reactions (3), are:

$$\mathbf{S_{cell}} = \begin{bmatrix} 1 & -1 & 0 & 0 & 0 & 0 & 0 & 0 & 0 & 0 & 0 & 0 & 0 \\ 0 & 0 & 1 & 1 & -1 & -1 & 0 & 0 & 0 & 0 & 0 & 0 & 0 \\ 0 & 0 & 0 & 0 & 0 & 0 & 1 & -1 & -1 & 0 & 0 & 0 & 0 \\ 0 & 0 & 0 & 1 & -1 & 0 & 0 & 0 & 0 & 1 & -1 & -1 & 1 \end{bmatrix}$$

$$\mathbf{S_{ext}} = \begin{bmatrix} 0 & 0 & 0 & 0 & 0 & 0 & 0 & 0 & 0 & 0 & 0 & 1 & -1 \end{bmatrix}.$$

The term $\mathbf{a(n)}$ in (4) is the associated vector of reaction propensities for the whole population of cells, with:

$$\mathbf{a(n)} = \left[\begin{array}{ccc|c} \mathbf{a(n)}^1 & \mathbf{a(n)}^2 & \vdots & \mathbf{a(n)}^N \end{array}\right.\left|\begin{array}{c} \\ \mathrm{d_{A_e}} n_5 \end{array}\right]^T$$

$$\mathbf{a(n)}^i = \left[\begin{array}{ccccccc} f(n_3^i, t) & \mathrm{d_I} n_1^i & \frac{\mathrm{C_R p_R}}{\mathrm{dm_R}} & \mathrm{k_{-1}} n_6^i & \frac{\mathrm{k_{-1}}}{\mathrm{k_{d1}}} n_2^i n_4^i & \mathrm{d_R} n_2^i & \frac{\mathrm{k_{-2}}}{\mathrm{k_{d2}}} (n_6^i)^2 \\ \mathrm{k_{-2}} n_3^i & \mathrm{d_{RA_2}} n_3^i & \mathrm{k_A} n_1^i & \mathrm{d_A} n_4^i & \mathrm{D} n_4^i & \mathrm{DV_c} n_5 & \end{array}\right]^T$$

Finally, $\mathcal{N}_{(\mathbf{JN+1})\times(\mathbf{JN+1})}$, where $J = 13$ is the number of reactions for the i^{th} cell, is a diagonal matrix of continuous normal random variables with zero mean and unit variance.

Notice we used lumped propensity functions derived from the reduced model, like the $f(n_3)$ Hill-like function associated to LuxI repression. This approach has already been used in (*44*). We validated it for our model by simulating the pseudo-reaction associated to $f(n_3^i)$ using CLE, and comparing the result with that obtained by simulating the set of

corresponding original reactions using Gillespie's direct method SSA (SI Section S.5).

Extrinsic noise was modeled by randomizing the values of the model parameters (*30*, *31*), an approach that can easily be integrated within the CLE framework. We assumed a normal distribution to generate the model parameters of the i^{th} cell in the population.

The stochastic simulations we performed for 400 min using $\delta t = 25 \cdot 10^{-4}$ sec.

Computational analysis

We used the stochastic model (4) of the proposed circuit, hereafter denoted as circuit QS/Fb, to explore the impact of some key circuit parameters on noise. As control circuit to compare with, we considered a second circuit which removes both QS and the feedback loop, denoted as NoQS/NoFb. For the computational analysis, this accounts to setting the synthesis of AHL to zero ($\mathrm{k_A} = 0\,\mathrm{min}^{-1}$) in model (4). This condition is achieved in the lab experimental implementation by taking out the gene coding for LuxI (Methods, Strains and plasmids). To asses the effect of cell-to-cell communication, we also considered a hypothetical circuit with feedback but without quorum sensing (NoQS/Fb, $\mathrm{D} = 0\,\mathrm{min}^{-1}$). Notice the circuit NoQS/Fb cannot actually be implemented for it assumes there is no diffusion of the autoinducer molecule across the cell membrane. Yet, it is useful as a computational thought experiment to account for the contribution of the cell-to-cell communication. Gene expression noise was evaluated using the squared coefficient of variation, i.e. the noise strength measure ($\eta^2 = (\sigma/\mu)^2$). This measure properly captures the contributions of both intrinsic and extrinsic noise (*45*), and allows comparisons for different expression rates.

We followed the following general procedure (depicted in SI Fig. S2). First, for different combinations of the model parameters, we performed temporal simulations of the number of molecules of each species in the circuit for every cell in the population of our system. Extrinsic noise was modeled by randomizing the values of the model parameters using a normal distribution with a variance of 15%. The models were implemented using OpenFPM (`http://openfpm.mpi-cbg.de`), a C++ version of the Parallel Particle Mesh (PPM) library

allowing efficient computational particle-mesh simulations (*46*). The code is available in (SI Section S.11). In all simulations we used a population of $N = 240$ cells in a culture volume of $10^{-3}\mu$l, corresponding to an optical cell density $\mathrm{OD}_{600} = 0.3$ (SI Section S.4). Cell density variations did not appreciably change the results, confirming the results in (*12*). The value of N used provided a good representative of a cell population, as confirmed by comparing with cell populations up to $N = 12000$ without significant variations in the population distributions obtained for the number of molecules expressed (SI Section S.6).

Then, we obtained the first two statistical moments μ and σ^2 for each species in the cell population at every time $\mathrm{t_k}$. We used the laws of total expectation and total variance. From these moments, we calculated long-term distributions to infer the noise strength of each species. To this end, we checked with our models that one realization of the population of N cells is enough to obtain unbiased values of the long-term moments of the population, provided there is enough time to perform the time average (SI Section S.4).

Finally, we generated noise strength maps for different sets of varying model parameters. We explored the effect of variations in parameters associated to expression of LuxI and LuxR, as they are as key parameters in our circuit. For LuxI, we considered the dissociation constant $\mathrm{k_{dlux}}$ between the transcription factor $(\mathrm{LuxR \cdot AHL})_2$ and the repressible $\mathrm{P_{lux}}$ promoter, the translation rate $\mathrm{p_I}$, and the basal expression α_I of the $\mathrm{P_{lux}}$ promoter. We sampled in the ranges $\mathrm{k_{dlux}} = [10 - 2000]$ molecules, $\alpha = [0.01 - 0.1]$, and $\mathrm{p_I} = [0.2 - 10]$ $\mathrm{min^{-1}}$ selected from the literature (*47–49*) and experimentally achievable in the lab. As for LuxR, we considered two values for the the translation rate $\mathrm{p_R}$: a strong RBS ($\mathrm{p_R} = 10$ $\mathrm{min^{-1}}$), and a medium-weak one ($\mathrm{p_R} = 2$ $\mathrm{min^{-1}}$). In addition, we analyzed the effect of different degradation rates $\mathrm{d_R}$ in the range $[0.02 - 0.2]$ $\mathrm{min^{-1}}$. For the case of the low mean scenario in Fig. 2 we included also simulations in the following range $\mathrm{p_I} = [0.004 - 0.02]$ $\mathrm{min^{-1}}$.

Notice from model (1) that although we only considered variations in the translation rates $\mathrm{p_I}$ and $\mathrm{p_R}$, these are tantamount to considering variations in the lumped values $\frac{\mathrm{C_I p_I}}{\mathrm{dm_I}}$, $\frac{\mathrm{C_R p_R}}{\mathrm{dm_R}}$ corresponding to the products of protein burst size, transcription rate and gene copy number.

We assumed variations in translation rates just because they are relatively simple to modify in a graded way by tuning the RBS (*47*), though also transcription rates could be easily tuned (*50*).

Strains and plasmids

To validate the *in silico* computational results, we implemented the QS/Fb and NoQS/NoFb circuits *in vivo*. We used components from the iGEM Registry of Standard Biological Parts. All parts were cloned using the Biobrick's foundation 3 Antibiotic Assembly method. All coding sequences have the double-terminator BBa_B0015, and were confirmed by sequencing. The circuit QS/Fb couples both QS-based cell-to-cell communication and the negative feedback subsystems. It was split in two subunits integrated in different plasmids.

On the one hand, plasmid pCB2tc contains the gene *luxR* (part BBa_C0062) coding for the protein LuxR constitutively expressed under the control of a medium strength promoter (part BBa_J23106), and a strong RBS (part BBa_B0034).
This insert was cloned into the pACYC184 plasmid cloning vector (p15A origin, 10-12 copies/cell, chloramphenicol/tetracycline (*51*)).

On the other hand, plasmid pYB06ta contains gene *luxI* (part BBa_C0161) under control of the P_{luxR} repressible promoter (part BBa_R0062) and a strong RBS (part BBa_B0034). The strong RBS BBa_B0034 and the green fluorescent protein (GFP, part BBa_E0040) were inserted using GIBSON assembly (NEB Catalog Number E2611S) upstream of *luxI*, right after the P_{luxR} promoter. This way, GFP, used as protein of interest (PoI in Fig. 1A) is co-expressed with LuxI.
They were inserted into the pBR322 plasmid cloning vector (pMB1 origin, 15-20 copies/cell, ampicillin/tetracycline (*51*)). Finally, both plasmids pCB2tc and pYB06ta were co-transformed in competent cells (DH-5α, Invitrogen). Notice being both plasmids low copy ones, they do not introduce a big metabolic burden on the cell. On the other hand, their variability is quite narrow so gene copy number will not be the only relevant extrinsic noise source in the

experimental setup.

As control network, we implemented the circuit NoQS/NoFb which removes both QS and the feedback loop. To this end, the plasmid pCB2tc above was co-transformed with the plasmid pAV02ta (pMB1 origin, ampicillin/tetracycline) containing only GFP downstream of the P_{luxR} repressible promoter (part BBa_R0062) and the the strong RBS (part BBa_B0034). Both were cloned in the pBR322 plasmid cloning vector.

All plasmids are shown in (SI Figs. S7, S8, S9) and are available at the ACS Synthetic Biology Registry as parts ACS_000551, ACS_000552, and ACS_000553.

Experimental protocol

For the experimental validation of the circuit (protocol details are in SI Section S.9), two sets of *E. coli* cells (cloning strain DH-5α) carrying the QS/Fb and NoQS/NoFb circuits respectively, were inoculated from -80^{o}C stocks into 3 mL of LB with appropriate antibiotics, followed by an overnight incubation at 37 ^{o}C and 250 rpm in 14 ml culture tubes. When the cultures reached an optical density (OD) of 4 (600 nm, Eppendorf BioPhotometer D30), the overnight cultures were diluted 500-fold (OD_{600} of 0.02) into M9 medium with appropriate antibiotics. These were used to inoculate new cultures, which were incubated for 7 hours (37^{o}C , 250 rpm,14 ml culture tubes) until they reached an OD_{600} between 0.2–0.3. At this point, cell growth and protein expression were interrupted by transferring the culture into an ice-water bath for 10 min. Next, 50 μL of each tube were transferred into 1 ml of phosphate-buffered saline with 500 μg/mL of the transcription inhibitor rifampicin (PBS + Rif) in one 5 mL cytometer tube, and incubated during 1 hour in a water bath at 37^{o}C, so that transcription kept blocked and GFP had time to mature and fold properly. Samples were measured at different time points using the BD FACSCalibur flow cytometer (original default configuration parameters), and flow cytometry data analyzed with custom scripts (SI Section S.10).

Acknowledgement

This work was partially supported by the Spanish Government (CICYT DPI2014-55276-C5-1) and the European Union (FEDER). Y.B. thanks grant FPI/2013-3242 of UPV. A.V. thanks I. Sbalzarini, E. Knust and the FACS Facility from the MPI-CBG and the ELBE Fellowship from the CSBD. Y.B. and A.V. thank for fruitful discussions on the algorithmic implementation and for the help with OpenFPM to Pietro Incadorna from Mosaic Group, CSBD, TU Dresden. The authors thank Christine Bäuerl for her help with the experimental implementation of the genetic circuit. The authors also thank Diego Oyarzún from Imperial College London for many insightful discussions about this topic.

Supporting Information Available

Supplementary Information accompanies this paper:

- Supplementary text
- Plasmid parts
- Software code

Competing financial interests: The authors declare no conflict of interest.

Author's contributions: Y.B., A.V., and J.P. designed research; Y.B., A.V., and J.P. performed research; Y.B., and A.V. performed experiment; Y.B., A.V., and J.P. analyzed data; and Y.B., A.V., and J.P. wrote the paper. Y.B.(Yadira Boada) and A.V. (Alejandro Vignoni) contributed equally to this work.

This material is available free of charge via the Internet at `http://pubs.acs.org/`.

References

1. Raser, J. M., and O'Shea, E. K. (2005) Noise in gene expression: origins, consequences, and control. *Science 309*, 2010–2013.

2. Raj, A., and van Oudenaarden, A. (2008) Nature, nurture, or chance: stochastic gene expression and its consequences. *Cell 135*, 216–226.

3. Labhsetwar, P., Cole, J. A., Roberts, E., Price, N. D., and Luthey-Schulten, Z. A. (2013) Heterogeneity in protein expression induces metabolic variability in a modeled Escherichia coli population. *Proceedings of the National Academy of Sciences 110*, 14006–14011.

4. Eldar, A., and Elowitz, M. B. (2010) Functional roles for noise in genetic circuits. *Nature 467*, 167–173.

5. Chalancon, G., Ravarani, C. N. J., Balaji, S., Martinez-Arias, A., Aravind, L., Jothi, R., and Babu, M. M. (2012) Interplay between gene expression noise and regulatory network architecture. *Trends Genet 28*, 221–32.

6. Jones, D. L., Brewster, R. C., and Phillips, R. (2014) Promoter architecture dictates cell-to-cell variability in gene expression. *Science 346*, 1533–6.

7. Kærn, M., Elston, T. C., Blake, W. J., and Collins, J. J. (2005) Stochasticity in gene expression: from theories to phenotypes. *Nat Rev Genet 6*, 451–64.

8. Tabbaa, O. P., Nudelman, G., Sealfon, S. C., Hayot, F., and Jayaprakash, C. (2013) Noise propagation through extracellular signaling leads to fluctuations in gene expression. *BMC Syst Biol 7*, 94.

9. Weber, M., and Buceta, J. (2013) Dynamics of the quorum sensing switch: stochastic and non-stationary effects. *BMC Syst Biol 7*, 6.

10. Tabareau, N., Slotine, J.-J. J., and Pham, Q.-C. C. (2010) How synchronization protects from noise. *PLoS Comput Biol 6*, e1000637.

11. Fuqua, C., Parsek, M., and Greenberg, E. (2001) Regulation of gene expression by cell-to-cell communication: acyl-homoserine lactone quorum sensing. *Annual review of genetics 35*, 439–468.

12. Tanouchi, Y., Tu, D., Kim, J., and You, L. (2008) Noise reduction by diffusional dissipation in a minimal quorum sensing motif. *PLoS Comput Biol 4*, e1000167.

13. Nelson, E. M., Kurz, V., Perry, N., Kyrouac, D., and Timp, G. (2013) Biological Noise Abatement: Coordinating the Responses of Autonomous Bacteria in a Synthetic Biofilm to a Fluctuating Environment Using a Stochastic Bistable Switch. *ACS synthetic biology 3*, 286–297.

14. Geiler-Samerotte, K. A., Bauer, C. R., Li, S., Ziv, N., Gresham, D., and Siegal, M. L. (2013) The details in the distributions: why and how to study phenotypic variability. *Curr Opin Biotechnol 24*, 752–9.

15. Müller, S., Harms, H., and Bley, T. (2010) Origin and analysis of microbial population heterogeneity in bioprocesses. *Curr Opin Biotechnol 21*, 100–13.

16. Fernandes, R. L. et al. (2011) Experimental methods and modeling techniques for description of cell population heterogeneity. *Biotechnol Adv 29*, 575–99.

17. Carlquist, M., Fernandes, R. L., Helmark, S., Heins, A.-L. L., Lundin, L., Sorensen, S. J., Gernaey, K., and Lantz, A. E. (2012) Physiological heterogeneities in microbial populations and implications for physical stress tolerance. *Microb Cell Fact 11*, 94.

18. Kim, K. H., and Sauro, H. M. (2012) Adjusting phenotypes by noise control. *PLoS Comput Biol 8*, e1002344.

19. Way, J. C., Collins, J. J., Keasling, J. D., and Silver, P. A. (2014) Integrating biological redesign: where synthetic biology came from and where it needs to go. *Cell 157*, 151–61.

20. Zechner, C., Seelig, G., Rullan, M., and Khammash, M. (2016) Molecular circuits for dynamic noise filtering. *Proceedings of the National Academy of Sciences* 201517109.

21. Zhang, C., Tsoi, R., and You, L. (2016) Addressing biological uncertainties in engineering gene circuits. *Integrative Biology 8*, 456–464.

22. Dublanche, Y., Michalodimitrakis, K., Kümmerer, N., Foglierini, M., and Serrano, L. (2006) Noise in transcription negative feedback loops: simulation and experimental analysis. *Mol Syst Biol 2*, 41.

23. Weber, M., and Buceta, J. (2011) Noise regulation by quorum sensing in low mRNA copy number systems. *BMC Syst Biol 5*, 11.

24. Russo, G., and Slotine, J. J. E. (2010) Global convergence of quorum-sensing networks. *Phys Rev E Stat Nonlin Soft Matter Phys 82*, 041919.

25. Vignoni, A., Oyarzún, D. A., Picó, J., and Stan, G. B. (2013) Control of protein concentrations in heterogeneous cell populations. *Procs. 2013 European Control Conference (ECC)* 3633–3639.

26. Zargar, A., Quan, D. N., and Bentley, W. E. (2016) Enhancing Intercellular Coordination: Rewiring Quorum Sensing Networks for Increased Protein Expression through Autonomous Induction. *ACS Synth Biol 5*, 923–8.

27. Egland, K. A., and Greenberg, E. P. (2000) Conversion of the Vibrio fischeri Transcriptional Activator, LuxR, to a Repressor. *Journal of Bacteriology 182*, 805–811.

28. Schaefer, A. L., Val, D. L., Hanzelka, B. L., Cronan, J. E., and Greenberg, E. P. (1996) Generation of cell-to-cell signals in quorum sensing: acyl homoserine lactone synthase

activity of a purified Vibrio fischeri LuxI protein. *Proceedings of the National Academy of Sciences 93*, 9505–9509.

29. Higham, D. J. (2008) Modeling and Simulating Chemical Reactions. *SIAM Review 50*, 347–368.

30. Joo, J., Plimpton, S. J., and Faulon, J.-L. L. (2013) Statistical ensemble analysis for simulating extrinsic noise-driven response in NF-ϒB signaling networks. *BMC Syst Biol 7*, 45.

31. Toni, T., and Tidor, B. (2013) Combined model of intrinsic and extrinsic variability for computational network design with application to synthetic biology. *PLoS Comput Biol 9*, e1002960.

32. Taniguchi, Y., Choi, P. J., Li, G.-W. W., Chen, H., Babu, M., Hearn, J., Emili, A., and Xie, X. S. (2010) Quantifying E. coli proteome and transcriptome with single-molecule sensitivity in single cells. *Science 329*, 533–8.

33. Potvin-Trottier, L., Lord, N. D., Vinnicombe, G., and Paulsson, J. (2016) Synchronous long-term oscillations in a synthetic gene circuit. *Nature 538*, 514–517.

34. Kaplan, H. B., and Greenberg, E. P. (1985) Diffusion of autoinducer is involved in regulation of the Vibrio fischeri luminescence system. *Journal of bacteriology 163*, 1210–1214.

35. Shih, Y.-P. P., Wu, H.-C. C., Hu, S.-M. M., Wang, T.-F. F., and Wang, A. H.-J. (2005) Self-cleavage of fusion protein in vivo using TEV protease to yield native protein. *Protein Sci 14*, 936–41.

36. Chen, X., Pham, E., and Truong, K. (2010) TEV protease-facilitated stoichiometric delivery of multiple genes using a single expression vector. *Protein Sci 19*, 2379–88.

37. Zhang, B., Rapolu, M., Liang, Z., Han, Z., Williams, P. G., and Su, W. W. (2015) A dual-intein autoprocessing domain that directs synchronized protein co-expression in both prokaryotes and eukaryotes. *Sci Rep 5*, 8541.

38. Swain, P. S., Elowitz, M. B., and Siggia, E. D. (2002) Intrinsic and extrinsic contributions to stochasticity in gene expression. *Proceedings of the National Academy of Sciences 99*, 12795–12800.

39. Hancock, E. J., Stan, G.-B. B., Arpino, J. A. J., and Papachristodoulou, A. (2015) Simplified mechanistic models of gene regulation for analysis and design. *J R Soc Interface 12*, 20150312.

40. Arpino, J. A. J., Hancock, E. J., Anderson, J., Barahona, M., Stan, G.-B. V. B., Papachristodoulou, A., and Polizzi, K. (2013) Tuning the dials of Synthetic Biology. *Microbiology 159*, 1236–53.

41. Chellaboina, V., Bhat, S., Haddad, W., and Bernstein, D. (2009) Modeling and analysis of mass-action kinetics. *IEEE Control Systems Magazine 29*, 60–78.

42. Mélykúti, B., Hespanha, J. a. P., and Khammash, M. (2014) Equilibrium distributions of simple biochemical reaction systems for time-scale separation in stochastic reaction networks. *J R Soc Interface 11*, 20140054.

43. Picó, J., Vignoni, A., Picó-Marco, E., and Boada, Y. (2015) Modelling biochemical systems: from Mass Action Kinetics to Linear Noise Approximation. *Revista Iberoamericana de Automática e Informática Industrial RIAI 12*, 241–252.

44. Woods, M. L., Leon, M., Perez-Carrasco, R., and Barnes, C. P. (2016) A statistical approach reveals designs for the most robust stochastic gene oscillators. *ACS Synth Biol*

45. Paulsson, J. (2004) Summing up the noise in gene networks. *Nature 427*, 415–8.

46. Sbalzarini, I. F., Walther, J. H., Bergdorf, M., Hieber, S. E., Kotsalis, E. M., and Koumoutsakos, P. (2006) PPM- A Highly Efficient Parallel Particle-Mesh Library for the Simulation of Continuum Systems. *Journal of Computational Physics 215*, 566–588.

47. Salis, H. M., Mirsky, E. A., and Voigt, C. A. (2009) Automated design of synthetic ribosome binding sites to control protein expression. *Nature biotechnology 27*, 946–950.

48. Egbert, R. G., and Klavins, E. (2012) Fine-tuning gene networks using simple sequence repeats. *Proceedings of the National Academy of Sciences of the United States of America*

49. Schmidl, S. R., Sheth, R. U., Wu, A., and Tabor, J. J. (2014) Refactoring and optimization of light-switchable Escherichia coli two-component systems. *ACS synthetic biology 3*, 820–831.

50. Brewster, R. C., Jones, D. L., and Phillips, R. (2012) Tuning promoter strength through RNA polymerase binding site design in Escherichia coli. *PLoS Comput Biol 8*, e1002811.

51. Sambrook et al., *Molecular cloning: a laboratory manual.*; Cold spring harbor laboratory press, 1989.

Graphical TOC Entry

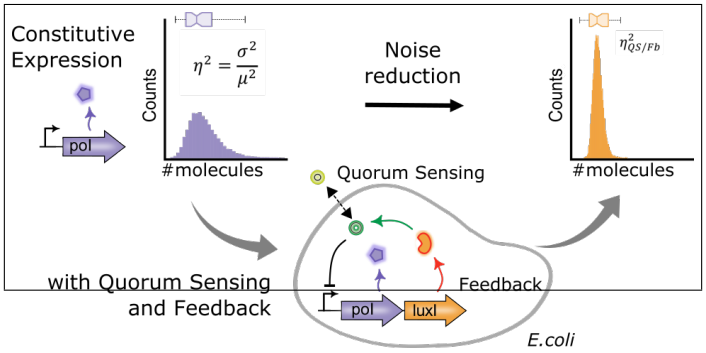

Controlling protein expression level is of interest in many applications. Yet, the stochastic nature of gene expression plays an important role and cannot be disregarded. We propose a gene synthetic circuit designed to control the mean gene expression in a population of cells and its variance. The circuit combines an intracellular negative feedback loop and quorum sensing based cell-to-cell communication system. Our *in silico* analysis using stochastic simulations reveals significant noise attenuation in gene expression through the interplay between quorum sensing and negative feedback, and explain their different roles for different noise sources. Preliminary *in vivo* results agree well with the computational results.